NJC

Accepted Manuscript

This is an *Accepted Manuscript*, which has been through the Royal Society of Chemistry peer review process and has been accepted for publication.

Accepted Manuscripts are published online shortly after acceptance, before technical editing, formatting and proof reading. Using this free service, authors can make their results available to the community, in citable form, before we publish the edited article. We will replace this *Accepted Manuscript* with the edited and formatted *Advance Article* as soon as it is available.

You can find more information about *Accepted Manuscripts* in the Information for Authors.

Please note that technical editing may introduce minor changes to the text and/or graphics, which may alter content. The journal's standard Terms & Conditions and the Ethical guidelines still apply. In no event shall the Royal Society of Chemistry be held responsible for any errors or omissions in this *Accepted Manuscript* or any consequences arising from the use of any information it contains.

ROYAL SOCIETY OF CHEMISTRY

www.rsc.org/njc

Journal Name

RSCPublishing

ARTICLE

Polyoxoanions assembled by condensation of Vanadate, Tungstate and Selenite: Solution Studies and Crystal Structures of Mixed Metal Derivatives $(NMe_4)_2Na_2[W^{VI}_4V^{V}_2O_{19}]\cdot 8H_2O$ and $(NMe_4)_{4.83}[(Se^{IV}W^{VI}_{4.57}V^{V}_{4.43}O_{33})_2(W^{VI}(O)(H_2O))(V^{V}O)_{2.6}]\cdot 10.57H_2O$

Cite this: DOI: 10.1039/xoxxoooooox

Received ooth January 2012,
Accepted ooth January 2012

DOI: 10.1039/xoxxoooooox

www.rsc.org/

Pavel A. Abramov*,[a,b] Eugenia V. Peresypkina,[a,b] Natalia V. Izarova,[c] Cristian Vicent,[d] Artem A. Zhdanov,[a] Nikolay B. Kompankov,[a] Tatiana Gutsul,[e] Maxim N. Sokolov [a,b]

Reaction of acidified aqueous solutions of Na_2WO_4, $NaVO_3$ and SeO_2 in 16:3:1 molar ratio gives a complex mixture of polyoxometalates (POMs) with both W^{VI} and V^{V} addenda, formulated as $[(Se^{IV}W^{VI}_xV^{V}_{9-x}O_{33})_2(W^{VI}O(H_2O))(VO)_m]^{n-}$ with x = 4, 5, 6; m = 2 or 3. In solution the sandwich-type complexes $[(Se^{IV}W^{VI}_xV^{V}_{9-x}O_{33})_2(W^{VI}O(H_2O))(VO)_m]^{n-}$ slowly lose Se and convert into $[V^{V}_2W^{VI}_4O_{19}]^{4-}$ and further to $[VW_5O_{19}]^{3-}$ with Lindqvist-type structure. These transformations were monitored with ^{51}V and ^{77}Se NMR, electrospray mass-spectrometry and capillary electrophoresis. Crystals of $(NMe_4)_2Na_2[(W_4V_2)O_{19}]\cdot 8H_2O$ (**1**) and $(NMe_4)_{4.83}[(SeW_{4.57}V_{4.43}O_{33})_2(W(O)(H_2O))(VO)_{2.6}]\cdot 10.57H_2O$ (**2**) were isolated and structurally characterized.

Introduction

Polyoxometalates (POM) constitute a large family of polynuclear oxo-hydroxo complexes of transition metals.[1] They are key compounds to many areas, such as catalysis [2], bioinorganic chemistry [3], organometallic chemistry [4] and materials science.[5,6] In particular vanadium-containing POMs are very good catalysts for numerous oxidation processes. Several research groups [7-9] studied oxidation of virtually all types of organic substrates by vanadium-containing POM under homogeneous conditions. Heterogeneous catalysis by V-containing POM as precursors also have found numerous applications.[10]

Mixed W / V POM have been known for a long time. Orange-yellow crystals of $M'_4[W_4V_2O_{19}]\cdot nH_2O$ and yellow $M'_3[W_5VO_{19}]\cdot nH_2O$ (M' = univalent cation) were obtained from stoichiometric mixtures of V(V) and W(VI) oxometalates. The $[W_4V_2O_{19}]^{4-}$ ion is stable in the pH range 4-7, while at pH 3 it converts into $[W_5VO_{19}]^{3-}$, which is stable in the pH range *ca*. 1-4. Above pH 4 it disproportionates into $[W_4V_2O_{19}]^{4-}$ and isopolytungstates.[11,12] The hexanuclear species with higher V : W ratio are unknown.

V-containing mixed Keggin anions $[XW_{11}V^{IV}O_{40}]^{n-}$ (X = P, Si, Ge, B, H_2, Zn), and $[XV^{IV}Mo_{11}O_{40}]^{n-}$ (X = P, Si) are intensely colored "heteropoly blues"-like species.[13] The comlex $[PW_{11}V^{IV}O_{40}]^{5-}$ is prepared by electrolytic reduction of the corresponding vanadium(V) complex, or by direct incorporation of VO^{2+} into $[PW_{11}O_{39}]^{7-}$ at pH 4.5.[14] Trivanadium(V)-substituted polyoxoanions $[A\text{-}\beta\text{-}H_xSiW_9V_3O_{40}]^{x-7}$ and $[\alpha\text{-}H_xP_2W_{15}V_3O_{62}]^{x-9}$ were synthesized from the trilacunary precursors $[A\text{-}\beta\text{-}SiW_9O_{34}]^{10-}$ and $[\alpha\text{-}P_2W_{15}O_{56}]^{12-}$.[15] A hybrid organometallic POM complex $(Bu_4N)_4[\{CpTi\}SiW_9V_3O_{40}]$ has been also synthesized.[16]

A related Dawson-type core $\{P_2W_{15}V_3\}$ can be grafted with an organic moiety by chelation of a tridentate ligand regioselectively to the $\{V_3\}$ cap.[17] Hasenknopf *et al.* reported a series of POM hybrids of the type $[P_2W_{15}V_3O_{59}\{(OCH_2)_2C(Et)NHCOR\}]^{5-}$, which are the first examples of amide insertion into a POM framework cage. The electron-acceptor properties of the POM in this case are transmitted to the ligand, which can be used in the design of POM-based redox sensors.[18] Self-assembly of weakly associated POMs driven by hydrogen-bonding interactions yielded a protein-sized tetramer, $[\{H_2NC(CH_2O)_3P_2W_{15}V_3O_{59}\}_4]^{24-}$, which is assembled from four $[H_2NC(CH_2O)_3P_2W_{15}V_3O_{59}]^{6-}$ subunits.[19] The reduced $[PMo_{12}O_{40}(V^{IV}O)_2]^{n-}$ anions, where vanadyl units are grafted onto reduced Keggin molybdophosphate, have been suggested as model compounds for spin qubits.[20, 21]

L. Cronin *et al.* investigated interaction of pyramidal heteroanions (SO_3^{2-} and TeO_3^{2-}) with mixed molybdate/vanadate addenda. These work has led to isolation of two novel Dawson-based complexes with sulfite, namely, $[Mo^{VI}_{11}V^{V}_5V^{IV}_2O_{52}(\mu_9\text{-}SO_3)]^{7-}$ and $[Mo^{VI}_{11}V^{V}_5V^{IV}_2O_{52}(SO_3)(Mo^{V}_6V^{V}O_{22})]^{10-}$,[22,23] whereas larger tellurite directed the self-assembly process towards the formation of

unique M_{24} cages, $[Mo^{VI}_{12}V^{V}_{8}V^{IV}_{4}Te^{IV}O_{69}(TeO_3)_2]^{10-}$ and $[Mo^{VI}_{12}V^{V}_{8}V^{IV}_{4}O_{69}(TeO_3)_2]^{14-}$, as well as {$M_{25}Te$} framework, $[Mo^{VI}_{11}V^{V}_{5}V^{IV}_{2}O_{52}(TeO_3)(Mo^{V}_{6}V^{V}O_{22})]^{10-}$.[24] The stereochemically active lone pair on the heteroanion imparts interesting redox and photophysical properties to the POM shell.[25,26] With SeO_3^{2-} L. Cronin isolated five new POM: $K_{10}[Mo^{VI}_{12}V^{V}_{10}O_{58}(SeO_3)_8]\cdot 18H_2O$, $K_7[Mo^{VI}_{11}V^{V}_{5}V^{IV}_{2}O_{52}(SeO_3)]\cdot 31H_2O$ and $(NH_4)_7K_3[Mo^{VI}_{11}V^{V}_{5}V^{IV}_{2}O_{52}(SeO_3)(Mo^{V}_{6}V^{V}O_{22})]\cdot 40H_2O$, the largest Mo/V–selenite-based POM reported to date $(NH_4)_{19}K_3[Mo^{VI}_{20}V^{V}_{12}V^{IV}_{4}O_{99}(SeO_3)_{10}]\cdot 36H_2O$, and $[Na_3(H_2O)_5\{Mo_{18-x}V_xO_{52}(SeO_3)\}\{Mo_{9-y}V_yO_{24}(SeO_3)_4\}]$.[27] In this work we focus on the VO_3^- /WO_4^{2-} /SeO_3^- system, with selenite as possible template for coordination of oxotungsten(VI) and oxovanadium(V) mixed addenda.

A reaction of $NaVO_3$ and H_2SeO_3 in water did not lead to any Se-containing polyvanadates. However, from CH_3CN such complexes have been isolated.[28] Recently the Cronin group reported characterization of a large selenite polytungstate family, of which the individual members are highly labile and coexist at very close pH values.[29] Addition of the vanadates to the WO_4^{2-} / SeO_3^- system could be expected to introduce more complexity. Partial substitution of vanadium for tungsten may affect the relative stability of various building blocks present in the virtual library of the selenopolymetalates. In this work we report self-assembly reactions between vanadate, tungstate and selenite under acidic conditions.

Results and discussion

Monitoring of the solution behavior

Mixing vanadate, tungstate and selenite in 16:3:1 molar ratio under acidic conditions (pH 1.5-2.0) gives a cherry-colored solution, which contains a mixture of different POMs. ^{51}V NMR spectra indicate the presence of two sharp peaks from $[W^{VI}_{5}V^{V}O_{19}]^{3-}$ (-522 ppm) and *cis*-$[W^{VI}_{4}V^{V}_{2}O_{19}]^{4-}$ (-523 ppm), as well as a very broad signal between -530 and – -590 ppm (see SI Fig. S9), which can be assigned to a mixture of $[(Se^{IV}W^{VI}_{x}V^{V}_{9-x}O_{33})_2(W^{VI}O(H_2O))(VO)_m]^{n-}$ polyanions with different x in the {$SeW_xV_{9-x}O_{33}$} fragments. After precipitation of enriching with Me_4NBr and repeated recrystallizations of the crude solids we still observed a complicated signal which was mainly combination of lines at -463, -528, -540 and -554 ppm (Fig. S10).

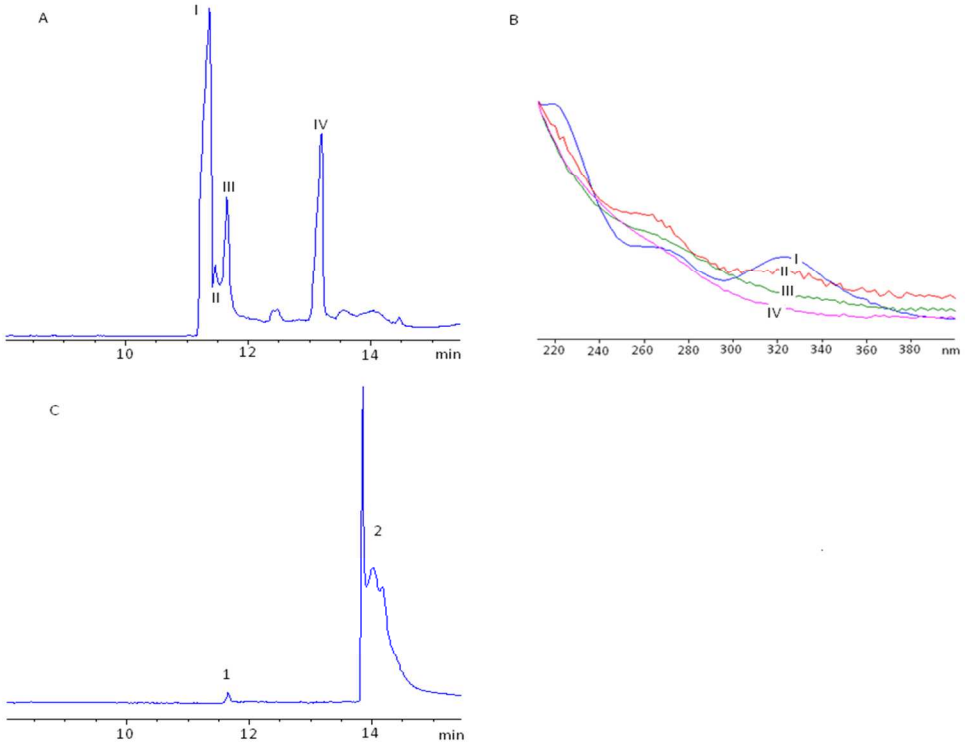

Fig. 1. A - electrophorogram of Na_2WO_4 solution. Peaks I – IV correspond to different polytungstates in solution. Conditions: silica capillary (L_{eff} = 52 cm), malonate electrolyte (0.1 M, pH = 2.8),U = -15kV, λ=250 nm, pneumatic injection (30 mbar·10 c); **B** – UV-VIS spectra of peaks I-IV recorded at on-line regime; **C** – electrophorogram of freshly mixed vanadate, tungstate and selenite under the same conditions.

The ^{77}Se NMR spectra show only a single broad signal centered at 1264 ppm, typical of a $\{Se^{IV}O_3\}$ unit, and therefore uninformative for elucidation of the structure of the species in solution. After repeated recrystallizations observe two signals in the ^{77}Se NMR spectra at 1408 and 1250 ppm for the bulk mixture of Me_4N^+ salts (Fig. S11).

In order to get more insight into the complexation processes in the SeO_3^{2-} / WO_4^{2-} / VO_4^{3-} (W / V / Se) system we applied capillary electrophoresis (CE) techniques. Initially we scanned a solution of pure Na_2WO_4 in malonate buffer (0.1 M, pH = 2.8) in order to check the polytungstate species present in such solutions (Fig. 1A). Four different forms were detected and identified by UV-vis spectra as I - $[W_{10}O_{32}]^{4-}$, II - α-$[H_2W_{12}O_{40}]^{6-}$, III β-$[H_2W_{12}O_{40}]^{6-}$, IV so-called ψ-metatungstate $[H_7W_{11}O_{40}]^{7-}$. (Fig. 1B). CE analysis of freshly prepared W / V / Se solution (molar ratio 16:3:1) (Solution A) is shown in Fig. 1C. The fastest-moving peak is due to β-$[H_2W_{12}O_{40}]^{6-}$ (marked as 1), while the second set of peaks appears as a group of poorly resolved peaks (marked as 2), corresponding to the species which all absorb at 400-450 nm (Fig. 2B). We assume that this group of peaks corresponds to differently charged forms of $[(Se^{IV}W^{VI}_xV^{V}_{9-x}O_{33})_2(W^{VI}O(H_2O))(VO)_m]^{n-}$ with various x. Such behavior is typical for species with close charge and hydrodynamic radii. Our assignment is supported by the fact that $[(Se^{IV}W^{VI}_xV^{V}_{9-x}O_{33})_2(W^{VI}O(H_2O))(VO)_m]^{n-}$ species and all polytungstates have distinctly different migration times, as shown in Fig. 2A and 2C. None of the vanadium-free polyoxotungstates formed in the Na_2WO_4 solution in the same medium absorbs light at 400 nm (Fig. 2B).

Electrophorograms of the reaction solution kept for two weeks at room temperature show three signals (Fig. 2A). The main signal (3) still corresponds to a mixture of $[(Se^{IV}W^{VI}_xV^{V}_{9-x}O_{33})_2(W^{VI}O(H_2O))(VO)_m]^{n-}$ polyanions with various W / V ratios, but they have shorter retention time than initially formed species. Logically, the species with higher W^{VI} content would move faster due to decrease of the negative charge. Therefore we suppose that with time these species are depleted in V and enriched in W. The minor signals 1 and 2 come from fast-moving compact anions of the Lindqvist type $[W^{VI}_xV^{V}_{6-x}O_{19}]^{n-}$. UV-vis spectra for each component are shown in Fig. 2B.

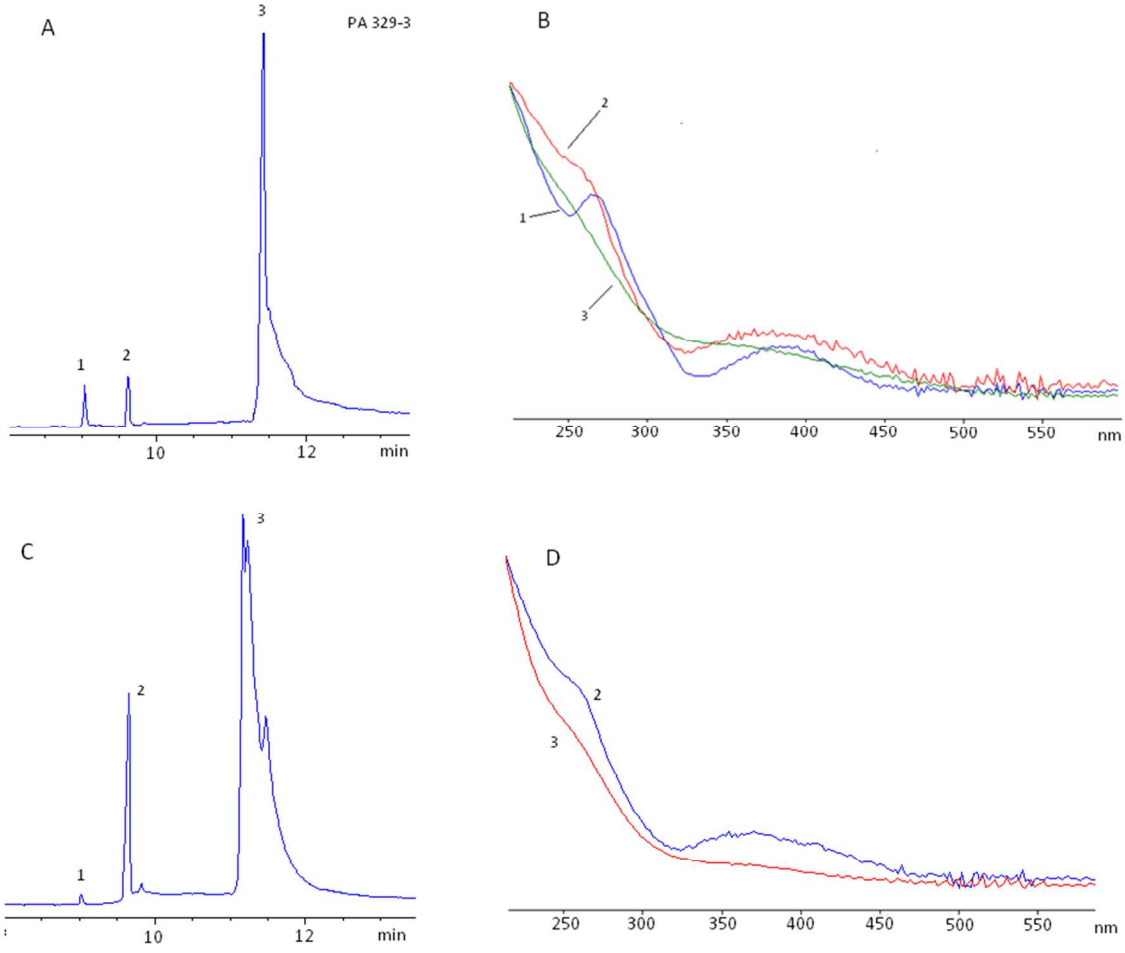

Fig. 2. A – electrophorogram of solution A after two weeks. CE conditions: silica capillary (L_{eff} = 40 cm), malonate buffer (0.1M, pH = 2.8), U = -15kV, λ = 254 nm, pneumatic injection from a solution (30 mbar·10c); **B** – UV-VIS spectra of peaks 1-3 at electrophorogram A from on-line regime; **C** – electrophorogram of A solution after one month (10^{-3} M); **D** – UV-VIS spectra of peaks 1-3 at electrophorogram C from on-line regime.

Journal Name RSCPublishing

ARTICLE

According to the UV-vis bands in CH_3CN at 217, 265 and 391 nm reported for $(Bu_4N)_3[W^{VI}_5V^{V}O_{19}]$ and $(Bu_4N)_3Na[W^{VI}_4V^{V}_2O_{19}]$ (209, 233 and 366 nm) [30] peak 1 is assigned to $[W^{VI}_5V^{V}O_{19}]^{3-}$ POM and peak 2 to $[W^{VI}_4V^{V}_2O_{19}]^{4-}$, in agreement with the rule that increase in the negative charge of a POM species with similar hydrodynamic radius increases retention time in the electrophorogram.

The same solution after one month (Fig. 2C) shows only a slight increase in the intensity of peak 2 ($[W^{VI}_4V^{V}_2O_{19}]^{4-}$). However after three months the peaks corresponding to $[(Se^{IV}W^{VI}_xV^{V}_{9-x}O_{33})_2(W^{VI}O(H_2O))(VO)_m]^{n-}$ polyanions virtually disappear, and the peak of $[W^{VI}_5V^{V}O_{19}]^{3-}$ (peak 1) becomes dominant. The electrophorogram also contains signals from species which have no absorption at 400 - 450 nm (peaks 3 - 5 in Fig. 3). Peak 3 probably corresponds to ψ-metatungstate $[H_7W_{11}O_{40}]^{7-}$, indicating release of free tungstate.

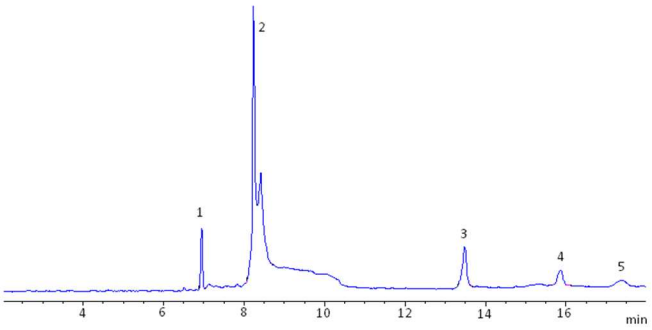

Fig. 3. Electrophorogram of solution A after 3 months. CE conditions: silica capillary (L_{eff}=40 cm), malonate electrolyte (0.1M, pH = 2.8), U = -15kV, λ=254 nm, pneumatic injection from a solution (30mbar·10c)

Calculation of the hydrodynamic radii

In order to confirm correct assignment of the peaks in CE plots based on UV-VIS data for each product (Fig. 2A), the values of the respective electrophoretic mobilities were calculated. The assessment was based on the charges found from the ESI-MS data (Fig. 4), and the viscosity of the electrolyte was assumed to be approximately equal to the viscosity of pure water (10^{-3} Pa·s). Estimated hydrodynamic radii of the anionic species in solution were calculated from the experimental migration times (t_i), after correction for the rate of the electroosmotic stream, full length of the capillary (L_Σ), effective length of the capillary (length from the capillary's enter to detector window, L_{eff}), and voltage (U).

The electrophoretic mobility (μ) can be explained from the experimental data: [31]

$$\mu_i = \frac{L_{eff} L_\Sigma}{t_i U} \quad (1),$$

Also μ can be found from the physical parameters of the system:

$$\mu_i = \frac{z_i F}{6\pi\eta r_i N_A} \quad (2)$$

when z_i – specific molecule charge, F – Faraday constant, η – electrolyte viscosity, r_i – hydrodynamic molecule radius, N_A – Avogadro constant.

Combination of equations 1 and 2 gives form for hydrodynamic radius of hydrated particle in the solution:

$$\mu_i = \frac{zF t_i U}{6\pi\eta r_i L_\Sigma L_{eff} N_A} \quad (3)$$

This equation was used to calculate radii of the particles corresponding to peaks 1, 2 and 3 (Fig. 2A). The results are summarized in the table 1.

Table 1. Values of the electrophoretic mobilities, hydrated particles radii and comparative radii for peaks 1,2 and 3 (Fig. 2A).

Peak number	electrophoretic mobility, $m^2/V{\cdot}s$	Radius of the hydrated particle, Å	Comparative radius (r_i/r_1)
1	$2{,}58{\cdot}10^{-8}$	6,60	1,00
2	$2{,}42{\cdot}10^{-8}$	7,02	1,06
3	$2{,}04{\cdot}10^{-8}$	8,35	1,26

These values give information that radius of the hydrated particle corresponding to peak 3 is 30% larger then to 1 or 2, which have approximately equal hydrodynamic radii. When compared with the anionic radii calculated from the structural data, which were 4.5 and 7 Å correspondingly, the hydrodynamic radii are typically higher, because of solvation. Based on this calculation we assign peak 3 to $[(Se^{IV}W^{VI}_xV^{V}_{9-x}O_{33})_2(W^{VI}O(H_2O))(VO)_m]^{n-}$ and peaks 1 and 2 to the W / V Lindqvist hexametalates.

Electrospray mass spectrometry

Electrospray ionization mass spectrometry (ESI-MS) is a valuable technique for POM characterization.[32] It has the potential to unravel complex reaction mixtures or to identify each separate component. For example, Cronin's group used ESI-MS to verify the molecular composition of Dawson-type POM with a single embedded heteroatom (P, Sb), where inherent disorder in the solid state made X-ray single crystal analysis ambiguous.[33]

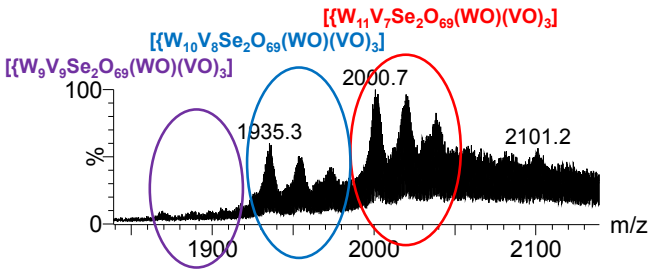

Fig. 4. Expanded regions of the ESI mass spectrum of 10-4 M water solution of a sample of 2 with 0.1 % of formic acid.

We used this technique in order to identify the ligand attached at the noble metal site in inherently disordered Keggin-type $[PW_{11}O_{39}M'L]^{n-}$ POM.[34]

For characterization of **2**, ESI-MS was expected to be particularly useful in order to specify the composition of both $\{SeM_9O_{33}\}$ ligands, as well as the variation in the W and V content and the central belt, in which either two or three VO groups can coexist. Owing to the propensity of highly charged POM to be ionized via multiple adduct formation with H^+ or alkali metal cations, which yields very crowded ESI mass spectra, we added a small amount of formic acid for enhancement of the abundancy of the H^+ adducts, thereby simplifying ESI mass spectra.[35]

This was crucial for unambiguous identification of the $[(Se^{IV}W^{VI}_xV^{V}_{9-x}O_{33})_2(W^{VI}O(H_2O))(VO)_m]^{n-}$ species. ESI mass spectrum is shown in Fig. S5, and an expanded region with peak assignments shown in Fig. 4.

Species featuring mixed metal $\{SeW_{9-x}V_xO_{33}\}$ moieties with the $\{WO(VO)_3\}$ central belt were dominant, as illustrated with the series of peaks in the m/z 1850 to 2100 range that corresponds to the adducts with H^+ and K^+ (see Figures S6, S7 and S8 for details).

The H_2O ligand from the $\{W^{VI}O(H_2O)\}$ fragment in the central belt was not observed upon ESI conditions most likely, because it is loosely bound to the W site. Species with the central $\{WO(VO)_2\}$ belt being inherently more negatively charged than those with the $\{WO(VO)_3\}$ belt were observed in the ESI mass spectrum as K^+ adducts and are overlapped with the dominant peaks. For example, species formulated as $\{[(Se_2W_{11}V_7O_{66})\{WO(VO)_2\}$ $+11H + 2K]^{2-}$ (m/z 2008.2) and $[(Se_2W_{10}V_8O_{66})\{WO(VO)_2\}$ $+ 10H + 2K]^{2-}$ (m/z 1941.2) were overlapped with the dominant peaks corresponding to $\{[(Se_2W_{11}V_7O_{66})\{WO(VO)_3\}$ $+10H]^{2-}$ and $\{[(Se_2W_{10}V_8O_{66})\{WO(VO)_3\}$ $+9H]^{2-}$ POMs with the central $\{WO(VO)_3\}$ belt at m/z 2000.7 and 1935.3, respectively. These results support the conclusion that crystals of **2** have: i) higher ratio of the species with $\{WO(VO)_3\}$ central belt than $\{WO(VO)_2\}$, and ii) the V content in the $\{SeW_{9-x}V_xO_{33}\}$ units encompasses x = 3, 4, and 5, which is reasonably in agreement with the crystal structure. Summarizing, the crystal structure of **2** is a solid solution of several similarly built Se-W-V POM, where one $\{WO\}^{4+}$ and two or three $\{VO\}^{3+}$ units coordinate two trilacunary $[SeW_{9-x}V_xO_{33}]^{n-}$ ligands, each of which can be $[SeW_6V_3O_{33}]^{11-}$, $[SeW_5V_4O_{33}]^{12-}$, or $[SeW_4V_5O_{33}]^{13-}$.

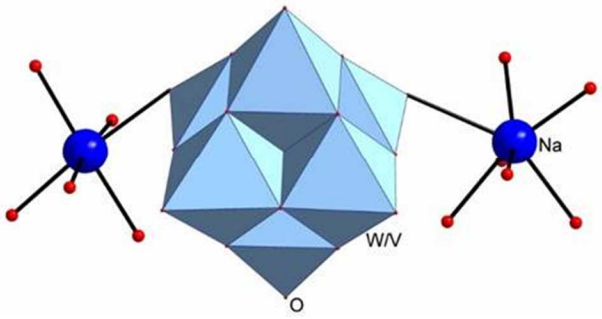

Fig. 5. The structure of heterometallic $[W_4V_2O_{19}]^{4-}$ Lindqvist anion in $(NMe_4)_2Na_2[W_4V_2O_{19}]\cdot 8H_2O$.

This means that $[SeW_9O_{33}]^{8-}$ allows replacement of as many as five species with higher vanadium tungsten atoms by vanadium. content should be inherently less stable because of too high negative charge. All these data suggest that self-assembly in the selenite-tungstate-vanadate system upon acidification involves initial formation of trilacunary $[SeW_{9-x}V_xO_{33}]^{n-}$ species with high vanadium content ($x \geq 5$). Their evolution involves assemblage into the sandwich-type structure via coordination $\{WO\}^{4+}$ and $\{VO\}^{3+}$ units and charge decrease by reducing V content (x = 3-5). These species are reasonably stable and can be isolated. However, over large periods of time (weeks and months) they decay with the formation of a mixture of $[W_5VO_{19}]^{3-}$ and $[W_4V_2O_{19}]^{4-}$, $[W_5VO_{19}]^{3-}$ becoming finally the dominant species.

Addition of NMe_4Br (TMABr) to the reaction solution gives, two types of crystals: yellow prisms of **1** and dark-red needles of **2**. Crystallization of **1** occurs after separation of **2**.

Crystal structures

Crystal structure of **1** corresponds to $(NMe_4)_2Na_2[W^{VI}_4V^{V}_2O_{19}]\cdot 8H_2O$ and contains Lindqvist anions $[W^{VI}_4V^{V}_2O_{19}]^{4-}$, where all metal positions are statistically occupied by W^{VI} and V^{V}. The charge balance is defined by the presence of four well distinguisheable countercations in the asymmetric unit, and ESI-MS analysis confirms the presence of $[W^{VI}_4V^{V}_2O_{19}]^{4-}$ single as single POM species in the crystals. Thus, a possible interpretation of the crystal structure as a solid solution of several Lindqvist species with different V/W content can be excluded. The positional isomerism of the $[W^{VI}_4V^{V}_2O_{19}]^{4-}$ anions results from different occupancies of W/V mixed positions. According to the refinement of the occupancies of W and V in every position, the overall content of V^{V} per Lindqvist anions is two atoms per anion, in agreement with CE data. Due to the disorder, the bond lengths involving M atom are averaged between W–O and V–O and are to be treated with care.

The M=O bond lengths with terminal oxygen atoms are 1.645(12)-1.710(11) Å, with M–μ_2-O bridging ones are in the range 1.881(7) - 1.935(7) Å. The central oxygen atom forms M–μ_3-O bonds in 2.257(8)-2.308(8) Å range (Table S2).

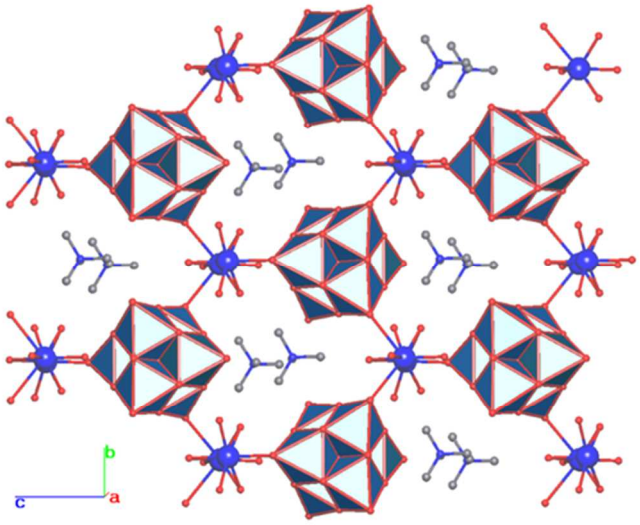

Fig. 6. Section of the hexagonal planer layer in $(NMe_4)_2Na_2[W_4V_2O_{19}]\cdot 8H_2O$.

Two sodium cations coordinate oxygen atoms of the anion via two terminal oxygen atoms (Fig. 5). The Na^+ cation with coordination number (CN) 6 forms shorter Na–O bond of 2.571(13) Å and the cation with CN = 7 a longer one, 2.831(13) Å. All other coordination sites at Na^+ ions are occupied by water molecules (Na–O 2.29(2)-2.507(18) Å). The $[W^{VI}_4V^{V}_2O_{19}]^{4-}$ anions and the $\{Na_2(H_2O)_{10}\}^{2+}$ cations form hexagonal planar layers (Fig. 6). The meshes of the layers are occupied by TMA^+ cations. The C–N bond distances within the TMA^+ are typical and lie in the range of 1.456(17)-1.499(18) Å. In the crystal packing the layers are shifted with respect to each other (Fig. S1). The interlayer space is occupied by TMA^+ cations and water of crystallisation.

Crystal structure of **2** corresponds to a solid solution formed by co-crystallized $[(Se^{IV}W^{VI}_xV^{V}_{9-x}O_{33})_2(W^{VI}O(H_2O))(VO)_m]^{n-}$ anions of similar structure, with variable *m* and average W / V composition of 4.57 / 4.43. The two $[SeW^{VI}_xV^{V}_{9-x}O_{33}]^{p-}$ fragments are coordinated by one $[W(O)(H_2O)]^{4+}$ unit and two or three oxovanadium $\{O=V\}^{3+}$ groups (Fig. 7) via terminal oxygen atoms. The metal positions within the $\{Se^{IV}M_9O_{33}\}$ ligands are mixed V^V and W^{VI} ones, while in the equatorial belts the positions in $[W(O)(H_2O)]^{4+}$ units and $\{V=O\}^{3+}$ groups are exclusively occupied by W and V, respectively.

The bond distances at the ordered metal sites are 1.68(3) Å for W=O, 2.28(2) Å for W–O_{H2O}, 1.52(4) - 1.58(2) Å for V=O, and 1.774(17)-1.97(2) Å for V–O. The averaged bond distances for (W/V)=O are 1.63(2)-1.68(2) Å and 1.82(2)-1.95(2) Å for (W/V)–O (Table S3). The POM anions lie on two-fold axis passing through the central V=O and the W=O groups. The two crystallographically independent positions of V atoms in the central belt of the polyanions have different occupancies. The central one lying on two-fold axis is occupied only in 60% of cases, while the second "peripheral" position is fully occupied. Therefore, one can propose two types of POMs to co-exist: one containing three V=O units (60%) and the other one with only two peripheral V=O units (40%) that co-crystallize due to minor difference in their structures within the same crystal (Fig. 7). The Me_4N^+ counter cations and solvated water molecules occupy their positions partly (total 4.85 cations per formula unit). Thus, if all the cationic positions were fully occupied, the structural type would accommodate six unipositive cations with corresponding re-distribution of the V / W content.

Conclusions

Our studies of SeO_3^{2-} / WO_4^{2-} / VO_4^{3-} system in aqueous acidic solutions with electrospray mass-spectrometry, capillary electrophoresis, UV-Vis spectroscopy and NMR reveal a complicated dynamics, which involves self-assembly of trilacunary $[SeW_{9-x}V_xO_{33}]^{n-}$ species with high vanadium content ($x \geq 5$). Their evolution in the solution involves self-assembly into the sandwich-type structure via coordination of $\{WO\}^{4+}$ and $\{VO\}^{3+}$ units and charge reduction by reducing V content (x = 3-5). These species are reasonably stable and can be isolated. Over large periods of time they decay to give a mixture of $[W_5VO_{19}]^{3-}$ and $[W_4V_2O_{19}]^{4-}$, $[W_5VO_{19}]^{3-}$ becoming finally the dominant species.

Experimental section

General information. All reagents were of commercial quality (Sigma Aldrich) and used as purchased. IR spectra (4000 – 400 cm^{-1}) were recorded on an IFS-85 Bruker spectrometer. ^{51}V and ^{77}Se NMR studies were carried out on a Bruker Avance 500 spectrometer with addition of very small amounts of D_2O at pH = 2 and at room temperature. The ^{51}V chemical shift was referenced to $VOCl_3$ (δ = 0 ppm) as external standard. The total sweep covers from –1000 to 0 ppm.

Capillary electrophoresis (CE) was carried out in Agilent G1600 CE-system with UV-detection. Analysis conditions are given below CE figures in the main text.

Electrospray Ionization mass spectrometry was performed on a Q-TOF premier mass spectrometer with an orthogonal Z-spray electrospray source (Waters, Manchester, UK). The temperature of the source block was set to 100°C and the desolvation temperature – to 200°C. A capillary voltage of 3.3 kV was used in the negative scan mode and the cone voltage was varied from low values Uc = 10 V (to control the extent of fragmentation of the identified species) to 60 V to observe the intrinsic gas-phase fragmentation channels. TOF mass spectra were acquired in the V-mode operating at a resolution of ca. 10000 (FWHM).

X-ray structural analysis. Crystallographic data and details of refinement for **1** and **2** are given in Table S1. All diffraction data were collected on a Bruker DUO CCD diffractometer with MoKα radiation (λ = 0.71073 Å) using φ and ω scans of narrow (0.5°) frames at 150 K. The structures were solved by direct methods and refined by full-matrix least-squares method against $|F|^2$ in anisotropic approximation using programs of SHELX family.[36] Absorption corrections were applied empirically using SADABS program.[37] All non-hydrogen atoms (with occupancy factors > 0.5 for light atoms) were refined anisotropically.

*Crystal structure of **1**.* The W / V content in all the positions of heavy atoms in POM was refined using FVAR instruction in SHELX.

Journal Name RSCPublishing

ARTICLE

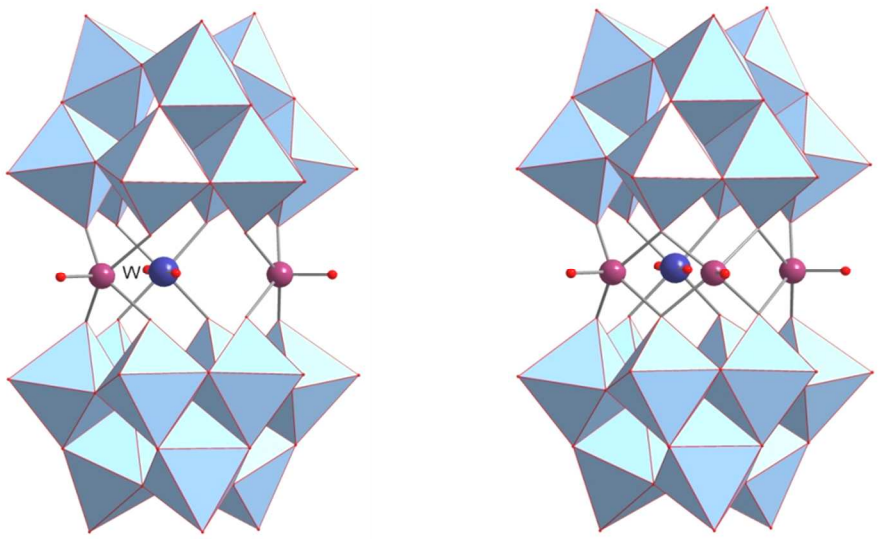

Fig. 7. The co-crystallized heterobimetallic $[(Se^{IV}W^{VI}_xV^{V}_{9-x}O_{33})_2(W^{VI}O(H_2O))(VO)_m]^{n-}$ anions, where m=2 (40%, left) and 3 (60%, right).

Due to correlations with overall scale factor, the refinement was unstable until the sum of occupation factors is constrained to the vanadium content. The latter was derived from the POM charge equal to the overall charge of counter cations. This estimation only became possible, because of ordered cationic portion in the crystal structure. The U_{iso} for W / V positions was set as 0.035 $Å^{-1}$; this value for displacement parameters and equated coordinates were used for every mixed position.

These constraints allowed the refinement to converge, and the resulted values for W content 0.81(3), 0.86(4), 0.57(3), 0.38(4) in positions W1 / V1, W2 / V2, W3 / V3 and W4 / V4 respectively were fixed, and the anisotropic refinement of displacement parameters was performed with equated coordinates of W and V for every position. The refined composition of the mixed positions can therefore be estimated as $W_{4.0(6)}/V_{2.0(6)}$ per formula unit. Water molecules coordinated to sodium cations are disordered, and the hydrogen atoms were not located.

Crystal structure of ***2***. The crystal of **2** proved to be a twin by merohedry (inversion twin), where the twin law is (1 0 0, 0 1 0, 0 0 -1) and the twin batches are refined to 0.91(2)/0.09(2). As a result of implemented twinning, the quality factors improved from R_1=0.0603, wR_2=0.1737, S=0.976 to R_1=0.0499, wR_2=0.1464, S=1.062. The W / V content in all positions of heavy atoms was refined step by step with U_{iso} = 0.05 $Å^{-1}$ for displacement parameters and coordinates constrained to be equal for the every mixed position.

The resulted values for W content are 0.55(5), 0.60(5), 0.66(6), 0.70(6), 0.73(7), 0.35(4), 0.33(4), 0.30(4) 0.35(4) and 1.00(1). The refined composition of the mixed positions can therefore be estimated as $W_{9.1(7)}/V_{8.9(7)}$ per formula unit. The independent refinement of occupancy factors for disordered cations gave a cationic content in good agreement with the resulted charge of POM anion.

We tried to isolate anions $[(Se^{IV}W^{VI}_xV^{V}_{9-x}O_{33})_2(W^{VI}O(H_2O))(VO)_m]^{n-}$ with the different cations ($Me_2NH_2^+$, K^+) to find conditions for the selective preparation of any $W^{VI}V^{V}$ species. The crystalline products isolated with the above-mentioned cations were studied with XRD analysis (some structural information is summarized in Table S4). Their crystal structures were solved and refined, but the correlations between occupancies of heavy atoms and overall scale factor, disorder of the cationic and sometimes anionic part of structure on one hand, and lack of chemical data on cationic and W / V content for a given crystal on the other, precluded finalization of the structure refinement. Therefore, only the type of the POM anions and the crystallographic data are reported in this manuscript. Further details for **1** and **2** may be obtained from the Cambridge Crystallographic Data Centre on quoting the depository numbers CCDC 1027881 and 1028644, respectively. Copies of this information may be obtained free of charge from http://www.ccdc.cam.ac.uk.

Self-assembly generation of Se / W / V species: Solution **X** was prepared by dissolving of $Na_2WO_4{\cdot}2H_2O$ (16.0 g, 48 mmol) in 20 ml of hot water. Solution **Y** was obtained by dissolving of $NaVO_3{\cdot}2H_2O$ (2 g, 12 mmol) in 10 ml of hot water. Then 1.0 g (9 mmol) of SeO_2 was added to the solution **Y**, the solutions **X** and **Y** were mixed, and pH value of the mixture was adjusted to 4 with HCl. The mixture was kept at 80 °C for an hour and then its pH value was brought to 2 with conc. HCl; the solution turned dark-red. After cooling the products were studied with NMR. ^{51}V NMR spectra at pH 1.5 –

2 indicate the presence of two groups of signals – sharp peaks from $[W^{VI}_5V^{V}O_{19}]^{3-}$ (-522 ppm) and *cis*-$[W^{VI}_4V^{V}_2O_{19}]^{4-}$ (-523 ppm), and a very broad peak between -530 – -590 ppm corresponding to and $[(Se^{IV}W^{VI}_xV^{V}_{9-x}O_{33})_2(W^{VI}O(H_2O))(VO)_m]^{n-}$ complexes. In order to crystallize anionic Se / W / V species, solid NMe_4Br (5.0 g, 0.032 mol) was added to the reaction mixture. After keeping this solution for 12 hours at 4 °C a mixture of predominantly yellow (**1**) and red (**2**) crystals were separated (ca 5 g of the solid material). Recrystallization of this solid from water gives red plates of **2** (yield of the solid sample around 1 g after several (2-4) fractional crystallizations, UC parameters of red plate and prism are identical with those of **2**, XPS analysis of final solid gives Se:W:V = 0.04:0.60:0.15).

Acknowledgements

The work was partially supported by RFBR grant 08-03-90109, President of Russian Federation grant for Scientific schools SS-516.2014.3 and President of Russian Federation fellowship for PAA. The authors also are grateful to the Serveis Centrals d'Instrumentació Científica (SCIC) of the Universitat Jaume I for providing us with mass spectrometry.

Notes and references

[a] Nikolaev Institute of Inorganic Chemistry SB RAS, Novosibirsk, Russia, 630090.
[b] Novosibirsk State University, Novosibirsk, Russia, 630090.
[c] Peter Grünberg Institute – PGI 6, Forschungszentrum Jülich, D-52425 Jülich, Germany.
[d] Serveis Centrals d'Instrumentació Científica, Universitat Jaume I, Av. Sos Baynat s/n, 12071 Castelló, Spain.
[e] Gitsu Institute of Electronic Engineering and Nanotehnologies, Academy of Sciences of Moldova, Academiei str. 3/3, Chisinau, MD-2028 Republic of Moldova.

Electronic Supplementary Information (ESI) available: Structural information, ESI-MS data, ^{51}V and ^{77}Se NMR data. See DOI: 10.1039/b000000x/

1 M.T. Pope, Heteropoly and Isopoly oxometalates, Springer, Berlin, Heidelberg, 1983; Polyoxometalates: From Platonic Solids to Anti-Retroviral Activity, ed. M. T. Pope and A. Müller, Kluwer Academic Publishers, Dordrecht, Netherlands, 1994.
2 H. Lu, Y.V. Geletii, C. Zhao, J.W. Vickers, G. Zhu, Z. Luo, J. Song, T. Lian, D.G. Musaev, C.L. Hill, *Chem. Soc. Rev.*, 2012, 41, 7572.
3 a) J.T. Rhule, C.L. Hill, D.A. Judd, *Chem. Rev.*, 1998, **98**, 327; b) B. Hasenknopf, Polyoxometalates: introduction to a class of inorganic compounds and their biomedical applications, *Front. Biosci.,* 2005, **10**, 275.
4 A. Dolbecq, E. Dumas, C.R. Mayer, P. Mialane, *Chem. Rev.,* 2010, **10**, 6009.
5 a) M. Ammam, *J. Mater. Chem. A*, 2013, **1**, 6291; b) Z. Li, X. Huang, X. Zhang, L. Zhanga, S. Lin, *J. Mater. Chem.*, 2012, **22**, 23602.
6 K.M. Seemann, A. Bauer, J. Kindervater, M. Meyer, C. Besson, M. Luysberg, P. Durkin, W. Pyckhout-Hintzen, N. Budisa, R. Georgii, C.M. Schneider, P. Kögerler, *Nanoscale*, 2013, **5**, 2511.
7 R. Neumann, *Inorg. Chem.,* 2010, **49**, 3594.
8 I.A. Weinstock, *Chem. Rev.*, 1998, **98**, 113.
9 a) Y. Kikukawa, Y. Kuroda, K. Suzuki, M. Hibino, K. Yamaguchia, N. Mizuno, *Chem. Commun.*, 2013,**49**, 376; b) Y. Ogasawara, S. Uchida, T. Maruichi, R. Ishikawa, N. Shibata, Y. Ikuhara, N. Mizuno, *Chem. Mater.*, 2013, **25**, 905; c) T. Yamaura, K. Kamata, K. Yamaguchi, N. Mizuno, *Catal. Today*, 2013, **203**, 76.
10 a) M.A. Alotaibi, E.F. Kozhevnikova, I.V. Kozhevnikov, *Appl. Cat. A,* 2012, **447–448**, 32; b) M. Craven, R. Yahya, E. Kozhevnikova, R. Boomishankar, C.M. Robertson, A. Steiner, I. Kozhevnikov, *Chem. Commun.*, 2013, **49**, 349; c) V.V. Costa, K.A.S. Rocha, I.V. Kozhevnikov, E.F. Kozhevnikova, E.V. Gusevskaya, *Catal. Sci. Technol.*, 2013, **3**, 244.
11 C.M. Flynn, M.T. Pope, *Inorg. Chem.*, 1971, **10**, 2524.
12 M.A. Leparulo-Loftus, M.T. Pope, *Inorg. Chem.*, 1987, **26**, 2112.
13 J.J. Altenau, M.T. Pope, R.A. Prados, H. So, *Inorg. Chem.*, 1975, **14**, 417.
14 D.P. Smith, H. So, J. Bender, M.T. Pope, *Inorg. Chem.*, 1973, **12**, 685.
15 R.G. Finke, B. Rapko, R.J. Saxton, P.J. Domaille, *J. Am. Chem. Soc*., 1986, **108**, 2947.
16 R.G. Finke, B. Rapko, P.J. Domaille, *Organometallics* 1986, **5**, 175.
17 C.P. Pradeep, D.-L. Long, G. N. Newton, Y.F. Song, L. Cronin, *Angew. Chem. Int. Ed.,* 2008, **47**, 4388.
18 J. Li, I. Huth, L. M. Chamoreau, B. Hasenknopf, E. Lacte, S. Thorimbert, M. Malacria, *Angew. Chem. Int. Ed.,* 2009, **48**, 2035.
19 E.F. Wilson, H. Abbas, B. J. Duncombe, C. Streb, D.-L. Long, L. Cronin, *J. Am. Chem. Soc.*, 2008, **130**, 13876.
20 J. Lehmann, A. Gaita-Ario, E. Coronado, D. Loss, *Nat. Nanotechnol.* 2007, **2**, 312.
21 D.-L. Long, R. Tsunashima, L. Cronin, *Angew. Chem. Int. Ed.*, 2010, **49**, 1736.
22 H.N. Miras, D.J. Stone, E.J.L. McInnes, R.G. Raptis, P. Baran, G.I. Chilas, M.P. Sigalas, T.A. Kabanos, L. Cronin, *Chem. Commun.*, 2008, 4703.
23 H.N. Miras, M.N.C. Ochoa, D.L. Long, L. Cronin, *Chem. Commun.*, 2010, **46**, 8148.
24 M.N. Corella-Ochoa, H.N. Miras, A. Kidd, D.-L. Long, L. Cronin, *Chem. Commun*., 2011, **47**, 8799.
25 D.-L. Long, Y.-F. Song, E. F. Wilson, P. Kögerler, S.-X. Guo, A. M. Bond, J. S. J. Hargreaves, L. Cronin, *Angew. Chem. Int. Ed.*, 2008, **47**, 4384.
26 N.I. Kapakoglou, P.I. Betzios, S.E. Kazianis, C.E. Kosmidis, C. Drouza, M.J. Manos, M.P. Sigalas, A.D. Keramidas, T.A. Kabanos, *Inorg. Chem.*, 2007, **46**, 6002.
27 M.N. Corella-Ochoa, H.N. Miras, D.-L. Long, L. Cronin, *Chem. Eur. J.*, 2012, **18**, 13743.
28 H. Nakano, T. Ozeki, A. Yagasaki, *Inorg. Chem.*, 2001, **40**, 1816.
29 J. Gao, J. Yan, S. Beeg, D.-L. Long, L. Cronin, *J. Am. Chem. Soc.*, 2013, **135**, 1796.
30 J. Tucher, S. Schlicht, F. Kollho, C. Streb, *Dalton,* 2014, **43**, 17029.
31 R. Kuhn, S. Hofstetter-Kuhn Capillary Electrophoresis: Principles and Practice // Springer-Verlag, 1993 - P.375.
32 a) H.N. Miras, E.F. Wilson, L. Cronin, *Chem. Comm.*, 2009, 1297; b) C.A. Ohlin, *Chem. Asian J.*, 2012, **7**, 262.
33 D.-L. Long, C. Streb, Y.F. Song, S. Mitchell, L. Cronin, *J. Am.Chem. Soc*., 2008, **130**, 1830.

34 a) M.N. Sokolov, S.A. Adonin, P. L. Sinkevich, C. Vicent, D.A. Mainichev, V.P. Fedin, *Dalton*, 2012, **41**, 9889; b) M.N. Sokolov, S.A. Adonin, D.A. Mainichev, P.L. Sinkevich, C. Vicent, N.B. Kompankov, A.L. Gushchin, V.A. Nadolinny, V.P. Fedin, *Inorg. Chem.* 2013, **52**, 9675; c) M.N. Sokolov, S.A. Adonin, P.L. Sinkevich, C. Vicent, D.A. Mainichev, V.P. Fedin, *Z. Anorg. Allg. Chem.*, 2014, **640**, 122.
35 a) R. Llusar, I. Sorribes, C. Vicent, *J. Clust. Sci.*, 2009, **20**, 177; b) M.T. Ma, T. Waters, K. Beyer, R. Palamarczuk, P.J.S. Richardt, R.A.J. O'Hair, A.G. Wedd, *Inorg. Chem.*, 2009, **48**, 598; c) C. Vicent, S.A. Adonin, A.V. Anyushin, D.A. Mainichev, M.N. Sokolov, *Eur. J. Inorg. Chem.*, 2014, **2014**, 5618.
36 G. Sheldrick, *Acta Cryst. ser. A.*, 2008, **64**, 112.
37 *APEX2, SAINT, and SADABS*, Bruker Advanced X-ray Solutions, Bruker AXS Inc., Madison, Wisconsin, USA, 2013.